

NLO properties of polythiophenes galvanostatically electrodeposited on ITO glasses

V. FIGA, J. LUC^a, M. BAITOUL^b, B. SAHRAOUI^{a,*}

Department of Chemical, Process and Materials Engineering, University of Palermo, Viale delle Scienze- Ed.6, 90128 Palermo, Italy

Laboratory POMA, UMR CNRS 6136, University of Angers, 2 Bd Lavoisier, 49045 Angers, France

^bFaculty of Science Dhar el Mahraz, BP1796, Fès 30 000, Morocco

A study of nonlinear optical properties of ClO₄⁻-doped polythiophenes, galvanostatically electrodeposited on ITO glasses, was carried out using second and third harmonic generation measurements. The effect of the oxidation state of the polymeric films was studied by comparing the nonlinear optical response of oxidised and reduced polythiophenes. Reduced polymeric films show higher values of the second and third order susceptibilities and a lower absorbance in respect to the oxidised ones. The morphology of the polythiophene films was studied by scanning electron and atomic force microscopes.

(Received June 22, 2008; accepted June 30, 2008)

Keywords: Polythiophene, SHG, THG, NLO properties

1. Introduction

Organic materials have been considered as promising candidates for various nonlinear optical (NLO) applications. With the advent of optical fibers in telecommunications in the late 1970s, practical applications for NLO devices operating on the basis of electro-optic (EO) effect become a serious aim. Polymeric EO materials can function as tunable Bragg wavelength filters, ultra-high bandwidth signal modulators for telecommunications, electrical-to-optical signals transducers, phase controllers of radiofrequency, etc. Their application is not only limited to the field of telecommunications. Indeed, polymeric materials with large second ($\chi^{(2)}$) and third order susceptibilities ($\chi^{(3)}$) are potentially applicable to optical data storage, optical computing, imaging, or dynamic holography. Other additional potential applications based on nonlinear phenomena, such as second harmonic generation (SHG) and third harmonic generation (THG), phase conjugation and optical bistability, may be also considered [1-5]. Experiments carried out on polythiophenes (PTs) [6] and their derivatives have shown that PTs present a large and very fast NLO response [7, 8]. In this field, we studied the influence of the oxidation state on the NLO properties of some selected polythiophenes, galvanostatically electrodeposited on ITO glasses.

2. Experimental

Polythiophene thin films were prepared electrochemically by anodic oxidation of the monomer. The electropolymerization of thiophene was performed using a three electrodes cell connected to a multichannel

potentiostat (VMP2, Princeton Applied Research). The working electrode was indium doped-tin oxide (ITO) glass ($R \leq 7 \Omega \text{cm}^{-2}$; thickness= 1.1 mm, Praezisions Glas & Optik GmbH), the counter electrode and reference were platinum and saturated calomel electrode (SCE), respectively. Thiophene (99.5%, Aldrich) was dissolved in acetonitrile (99%, Aldrich) HPL grade anhydrous and 0.1M lithium perchlorate (99.9%, Aldrich) was used as supporting electrolyte for both giving the solvent an electrical conductivity and furnishing the dopant anions for the polymeric matrix. The monomer concentration was 0.1 mol/L. Before the electropolymerization, ITO glasses were sonicated in acetone for 10 minutes. Electropolymerization was performed galvanostatically applying a constant current density of 0.8 mAcm^{-2} . In order to investigate on the possible dependence of the NLO properties with the oxidation state, two kinds of samples were prepared: oxidised and reduced polythiophenes. All the samples differ for the circulated charge during the electrodeposition (from 90 to 380 mCcm^{-2}). For the reduced samples, the reduction charge was 90 mCcm^{-2} (see Table 1) and the applied current density was 0.5 mAcm^{-2} . The films were removed from the solution, washed in distilled water and dried in air. The measurements of the experimental thickness were carried out using a profilometer (Dektak 6M Veeco) and the UV-Visible spectra were recorded between 300 and 1100 nm by a Spectrometer (Lambda 19 Perkin Elmer).

SHG measurements were carried out using the Maker fringes technique [9] at 1064 nm and for the *s-s* polarization state (see Fig. 1). The quartz *y*-cut plate ($\chi^{(2)} = 1 \text{ pmV}^{-1}$ [10]) has been used as reference material for SHG and the fused silica plate ($\chi^{(3)} = 0.02 \times 10^{-20} \text{ m}^2 \text{V}^{-2}$ [11]) for THG measurements.

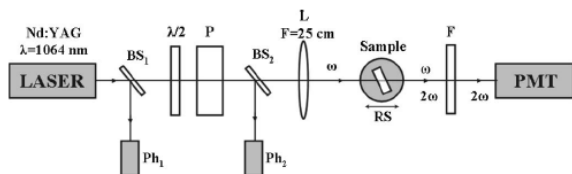


Fig. 1. Experimental set up for SHG measurements: (BS_1 , BS_2) beam splitters, (Ph_1 , Ph_2) photodiodes, ($\lambda/2$) half-wave plate, (P) Glan polarizer, (L) convergent lens, (RS) rotation stage, (F) filter(s), and (PMT) photomultiplier tube.

As a fundamental beam, we used the output beam of a Q-switched Nd:YAG laser (Quantum Elite), generating a coherent beam at $\lambda=1064$ nm with 16 ps pulse duration and 10 Hz repetition rate. A half-wave plate seated before the polarizer to control the polarization and the power density of the fundamental beam. The intensity at the input of the sample is assumed to be spatio-temporal Gaussian distribution. The beam diameter was 0.5 mm on the film and the applied power density was 5 GWcm^{-2} . After the sample, a selective filter was placed to select the harmonic wave (at 532 nm for SHG or 355 nm for THG) before the photomultiplier (Hamamatsu R1828-01). Lastly, the morphology of the polythiophene thin films was investigated using a scanning electron microscope (SEM) and an atomic force microscope (AFM). All the experiments were performed at room temperature.

3. Results and discussion

3.1. Polythiophene electrodeposition

The electrodeposition of polythiophene films on ITO glasses is produced by anodic oxidation of the neutral monomer. One molecule of monomer requires two electrons for being oxidised. The mechanism proposed for the electropolymerization of heterocycles [12-14], is constituted by different electrochemical and chemical steps. The first electrochemical step is the monomer oxidation to its radical cation. The second step involves the coupling of two radicals to produce a dihydro-dimerization which leads to a neutral dimer after a reaction of deprotonation. Due to the applied potential, the dimer, which is more easily oxidised than the monomer, occurs in its radical form and undergoes a further coupling with a monomeric radical. Electropolymerization proceeds until the oligomer becomes insoluble in the electrolytic medium and precipitates into the electrode surface.

The different samples were prepared applying a constant current density and stopping the electrodeposition after different circulated charges. The amount of mass that is electrodeposited on the working electrode surface is proportional to the circulated charge. The theoretical thickness of the polymeric film (t) can be determined by the Faraday's law:

$$t = \frac{qM\eta_F}{\rho AzF} \quad (1)$$

where q is the circulated charge, M the molar mass, F the Faraday's constant, ρ the density of the monomer, z the number of electrons involved in the electropolymerization reaction, and η_F the faradic efficiency.

By assuming that: $M = 84.14 \text{ g mol}^{-1}$, $F = 96480 \text{ C mol}^{-1}$, $\rho = 1.05 \text{ g cm}^{-3}$, $z = 2$ and $\eta_F = 1$, we obtained a theoretical thickness for the different circulated charges. By comparing the theoretical and experimental thicknesses, we calculated a faradic efficiency between 48 and 81%. It means that during the electropolymerization process, not the whole current is employed in the film growth because parallel reactions take place. The conditions of preparation are summarized in table 1.

During the process of electropolymerization, the polymeric film includes anions from the electrolytic solution, in order to conserve the electro-neutrality. The growth is accompanied by the doping of the film. During the reduction process, anions move from the polymeric matrix to the solution, and a dedoping process occurs. The difference between the charge transferred during the electropolymerization and the reduction allows to carry out a qualitative evaluation of the doping level.

Table 1. Electropolymerization parameters: $Q_{\text{electropol}}$ is the charge circulated electropolymerization, and Q_{red} the charge circulated for the reduced samples.

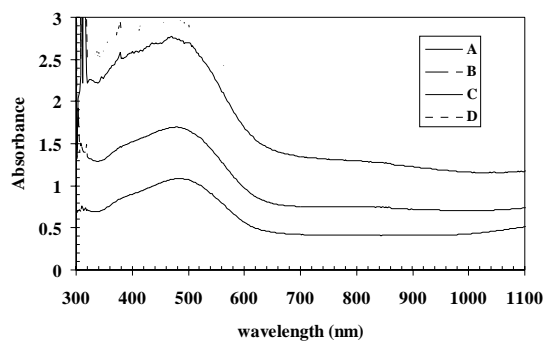
| Compound | $Q_{\text{electropol}}$ [mCcm ⁻²] | Q_{red} [mCcm ⁻²] | Theoretical thickness [nm] | Experimental thickness [nm] |
|----------|--|---|-------------------------------|--------------------------------|
| A | 95 | - | 393 | 190 |
| B | 190 | - | 786 | 580 |
| C | 284 | - | 1180 | 760 |
| D | 380 | - | 1570 | 1100 |
| E | 95 | 95 | 393 | 210 |
| F | 190 | 95 | 786 | 640 |
| G | 284 | 95 | 1180 | 650 |
| H | 380 | 95 | 1570 | 820 |

3.2. Absorption spectra

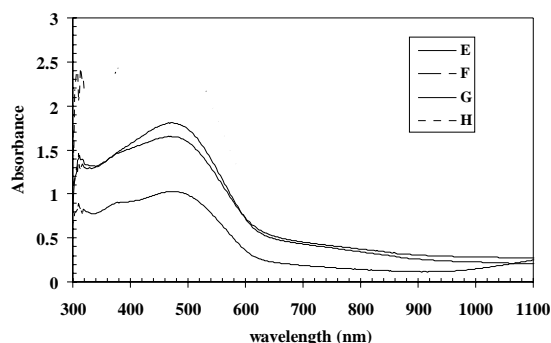
The interaction between light (UV/VIS) and a conjugated polymer causes the generation of charge carriers and the conduction of photogenerated charge carriers. The explanation of these phenomena is provided by the "exciton model". According to this model, the absorption of a photon by a conjugated polymer promotes an electron from the ground state to an upper electronically excited state, which takes the configuration of a quasi-particle and can be considered as an electron/hole pair.

The absorption spectra of the oxidised and reduced samples are showed in figure 2. High values of absorbance were found, due to the fact that the polymeric films are dark. The values of absorbance increase with the increasing of the thickness of films. For all the samples, the absorption occurs in the visible region, as we expected for conjugated polymers. The maximum absorption is

around 480 nm and the transition $\pi-\pi^*$ of compounds could be assigned to this wavelength. By comparing the samples prepared with the same circulated charge, the oxidised samples present a higher absorption. The values of the absorption coefficients at 532 nm and at 355 nm are reported in table 2.



a



b

Fig. 2. Absorption spectra of the electrodeposited polythiophenes (a: A-D and b: E-H).

3.3. Second harmonic generation experiments

SHG is a nonlinear optical process in which the fundamental beam at a frequency ω interacts with a nonlinear medium and results in the generation of an additional beam with frequency 2ω . The second-order susceptibility was calculated by comparing the SH intensity obtained for the samples and for a reference material (quartz y -cut). The average orientation of the compounds was estimated comparing the experimental results with the theoretical angular dependence of the SH intensity.

In figure 3, the SH intensity versus the incident angle for the compound F is reported as example. The SHG signal is symmetric with respect to 0° . The polythiophenes films show a maximum intensity at 45° with respect to the incident beam. It means that the chromophores are oriented perpendicularly to the surface. They assume a centro-symmetric configuration at 0° where the SHG signal is equal to zero.

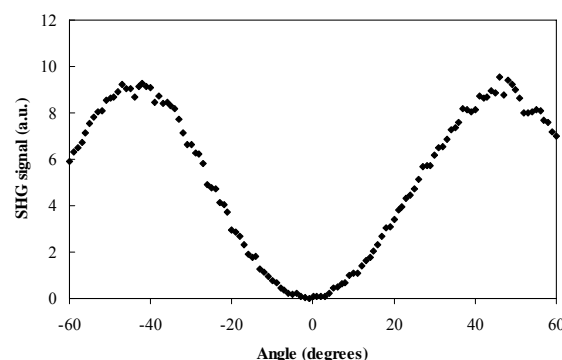


Fig. 3. SHG signal vs incident angle for the compound F.

For a fundamental beam of constant intensity and under the hypothesis of no dispersion, the second order nonlinear susceptibility is related with the $\chi^{<2>}$ of the reference material by the following equation [15]:

$$|\chi^{<2>}| = |\chi_Q^{<2>}| \left(\frac{2}{\pi} \right) \left(\frac{L_{C,Q}}{l} \right) \left(\sqrt{\frac{I_Q^{2\omega}}{I_Q^{2\omega}}} \right) \quad (2)$$

with:

$$L_{C,Q} = \frac{\lambda_\omega}{4 \times |n_{Q(2\omega)} - n_{Q(\omega)}|} \quad (3)$$

where $I^{2\omega}$ is the maximal SH intensity of the sample, $I_Q^{2\omega}$ the maximal SH intensity of quartz ($\approx 2.5 \times 10^5 \text{ W cm}^{-2}$), $L_{C,Q}$ is the coherence length of quartz ($\approx 20.5 \text{ }\mu\text{m}$), l the thickness of the sample, $\chi_Q^{<2>}$ the second order susceptibility of quartz (1.0 pmV^{-1}) [10], $n_{Q(2\omega)}$ the refractive index of second harmonic wave (1.547 at 532 nm) and $n_{Q(\omega)}$ the refractive index of fundamental wave (1.534 at 1064 nm) [16].

The values of $\chi^{<2>}$, summarized in table 2, were calculated by fitting the experimental SHG signals versus incident angle plots, by the equation (2).

Table 2. Second and third order susceptibilities, and linear absorption coefficients of the investigated samples

| Compound | $\chi_{eff}^{<2>}$ [pmV^{-1}] | $\chi_{elec}^{<3>}$ [$10^{-20} \text{ m}^2 \text{ V}^{-2}$] | $\alpha_{2\omega}$ [10^4 cm^{-1}] | $\alpha_{3\omega}$ [10^4 cm^{-1}] |
|--------------|---|--|--|--|
| A | 0.16 | 1.44 | 11.6 | 8.98 |
| B | 0.10 | 0.39 | 5.93 | 5.32 |
| C | 0.05 | 0.06 | 7.39 | 7.08 |
| D | 0.02 | 0.01 | 5.41 | 5.34 |
| E | 0.18 | 2.27 | 9.18 | 9.07 |
| F | 0.15 | 0.62 | 5.33 | 4.89 |
| G | 0.15 | 0.47 | 4.86 | 4.83 |
| H | 0.06 | 0.41 | 6.08 | 6.35 |
| Quartz | 1.0 | - | | |
| Fused silica | - | 0.02 | | |

The obtained parameters are higher in the case of the reduced samples and they decrease with thickness. A higher value of $\chi^{<2>}$ was found in the case of compound E. Figure 4 shows the superimposition of the values of the second order susceptibility for reduced and oxidised samples versus the electric charge circulated during the electropolymerization.

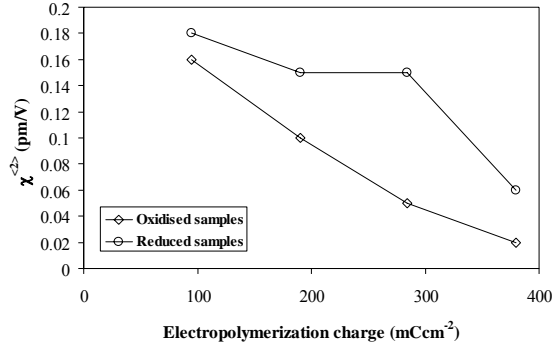


Fig. 4. Superimposition of $\chi^{<2>}$ vs the electropolymerization charge of the oxidised and reduced samples.

3.4. Third harmonic generation experiments

THG is a third order nonlinear optical process in which the fundamental beam at the frequency ω interacts with a nonlinear medium and another beam of frequency 3ω is generated. The third order susceptibility is the sum of different contributions belonging to different physical processes. It can be written as [17-18]:

$$\chi^{<3>} \approx \chi_{elec}^{<3>} + \chi_{mol}^{<3>} + \chi_{therm}^{<3>} + \chi_{stric}^{<3>} \quad (4)$$

where $\chi_{elec}^{<3>}$ is the electronic component, $\chi_{mol}^{<3>}$ the molecular (vibrational and rotational) component, $\chi_{therm}^{<3>}$ the thermal contribution, and $\chi_{stric}^{<3>}$ the electrostriction component. These contributions have different response times. For the THG measurements in picosecond regime, just the electronic contribution can be estimated. In Figure 5 is represented the THG signal for the compound A.

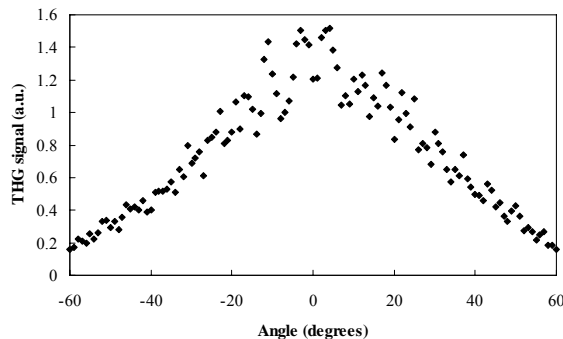


Fig. 5. THG signal vs incident angle for the compound A.

The model of Kubodera and Kobayashi [19] gives the $\chi_{elec}^{<3>}$ contribution of the medium by comparing, directly, its maximum of light intensity of third harmonic signal with that of the reference material, used for calibrating the experimental set up. In this model, both the refractive indices and the third order susceptibility are considered real, so the weak absorption of a nonlinear sample and the third order susceptibility to the substrate are neglected. The expression of $\chi_{elec}^{<3>}$ is given by the following equation:

$$\chi_{elec}^{<3>} = \chi_S^{<3>} \left(\frac{2}{\pi} \right) \left(\frac{L_{C,S}}{l} \right) \sqrt{\frac{I^{3\omega}}{I_S^{3\omega}}} \quad (5)$$

with:

$$L_{C,S} = \frac{\lambda_\omega}{4 \times |n_{S(3\omega)} - n_{S(\omega)}|} \quad (6)$$

where $\chi_S^{3\omega}$ is the third order nonlinear optical susceptibility of fused silica ($\chi_S^{3\omega} = 0.02 \times 10^{-20} \text{ m}^2 \text{V}^{-2}$ [11] at 1064 nm), l the thickness of the nonlinear material, $L_{C,S}$ the coherence length of fused silica ($\approx 6,7 \text{ }\mu\text{m}$), $I^{3\omega}$ the maximal TH intensity of the nonlinear material, $I_S^{3\omega}$ the maximal TH intensity of fused silica ($\approx 4.1 \text{ Wcm}^{-2}$), $n_{S(3\omega)}$ the refractive index of third harmonic wave (1.47617 at 355 nm) and $n_{S(\omega)}$ the refractive index of fundamental wave (1.44967 at 1064 nm) [20].

On considering that the linear absorption of the nonlinear material is not equal to zero ($\alpha > 0$), the equation (5) becomes:

$$\chi_{elec}^{<3>} = \chi_S^{<3>} \left(\frac{2}{\pi} \right) L_{C,S} \frac{\alpha/2}{1 - e^{-(\alpha l/2)}} \sqrt{\frac{I^{3\omega}}{I_S^{3\omega}}} \quad (7)$$

The values of $\chi_{elec}^{<3>}$, summarized in table 2, were calculated by fitting the experimental THG signals with the equation (5).

The obtained parameters are higher in the case of the reduced samples and they decrease with thickness. A value of $\chi_{elec}^{<3>}$ higher of two orders of magnitude was found in the case of compound E in respect to the reference material. Figure 6 shows the superimposition of the values of the third order susceptibility for reduced and oxidised samples versus the electric charge circulated during the electropolymerization.

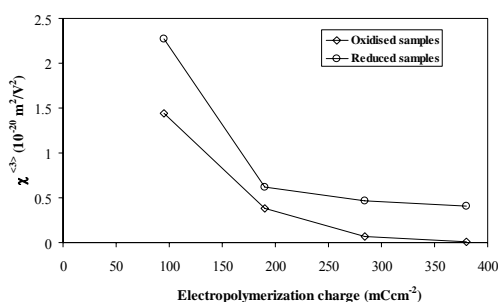


Fig. 6. Superimposition of $\chi^{(2)}$ vs the electropolymerization charge of the oxidised and reduced samples.

3.5. Morphological investigation

The morphology of the surface exposed to the electrolytic solution of the electrodeposited polythiophenes, was analyzed by SEM and AFM. At low magnifications the polymeric films show a compact structure. Figure 7 shows a SEM image of compound E. An ordered globular structure was observed in different regions of the sample. A diameter of approximately 200 nm was estimated for the agglomerates of the compound E.

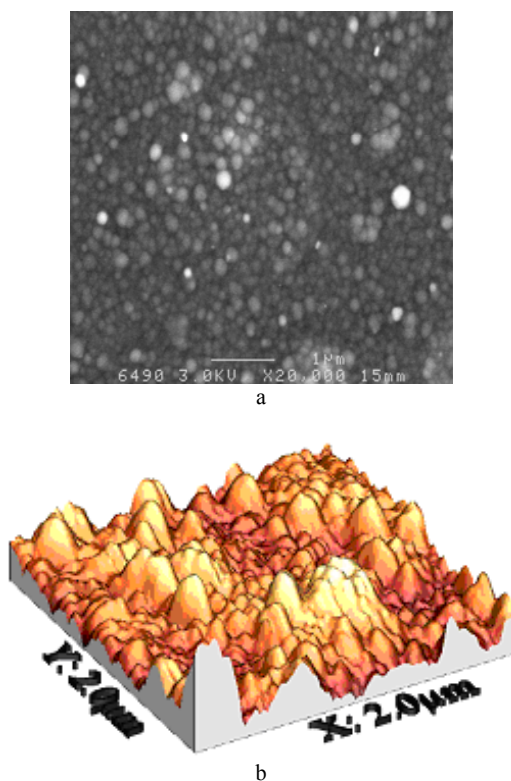


Fig. 7. Surface SEM ($15 \mu\text{m} \times 15 \mu\text{m}$) (a) and AFM ($2 \mu\text{m} \times 2 \mu\text{m}$) (b) morphologies of electrodeposited PT on ITO glass after reduction (compound E).

In order to complete the morphological analysis, a 3D study of the surface was performed. In figure 8 is shown an AFM image of the compound E. The surface appears to have a RMS roughness of approximately 17 nm.

4. Conclusions

A study of the influence of the oxidation state on the nonlinear optical properties of galvanostatically electrodeposited polythiophenes was performed. Different polythiophenes were prepared according to different charges circulated during the electropolymerization and according to different doping levels.

The second order NLO properties of ClO_4^- -doped polythiophenes were analyzed by the Maker fringes technique, using a fundamental beam of 1064 nm and the values of second order nonlinear susceptibilities were calculated compared with the reference material (γ -cut quartz). They seem to have higher values in the case of reduced samples and to depend on their thickness. The compound that shows a higher value of $\chi^{(2)}$ is the compound E, even if this value is negligible in respect to the reference material second-order susceptibility.

The third order nonlinear optical properties of these compounds were analyzed compared with the reference material (fused silica). Even in this case, we obtained higher values of the third order susceptibility for the reduced samples, particularly for the compound E. It has a lower thickness and a lower doping level than the other reduced compounds. It has a value of $\chi^{(3)}$ which is two order of magnitude higher than the reference material so it can be a promising material for the third order nonlinear optics applications.

In next works we will investigate, in a detailed way, on the possibility to increase $\chi^{(3)}$ values by further decreasing both the thickness and the doping level of this compounds.

Acknowledgements

The authors want to acknowledge the Service Commun d'Imagerie et Analyses Microscopiques (SCIAM) of University of Angers for performing AFM and SEM measurements.

References

- [1] A. Migalska-Zalas, J. Luc, B. Sahraoui, I.V. Kityk, *Opt. Mat.* **28**(10), 1147 (2006).
- [2] J. Luc, J. L. Fillaut, J. Niziol, B. Sahraoui, J. Optoelectron. Adv. Mater. **9**(9), 2826 (2007).
- [3] J. Luc, A. Migalska-Zalas, S. Tkaczyk, J. Andriès, J.-L. Fillaut, A. Meghea, B. Sahraoui, J. Optoelectron. Adv. Mater., Review paper, **10**(1), 29 (2008).
- [4] B. Kulyk, Z. Essaidi, J. Luc, Z. Sofiani, G. Boudebs, B. Sahraoui, V. Kapustianyk, B. Turko, J. Appl. Phys., **102**(113113) 1 (2007).

- [5] W. Bi, N. Louvain, N. Mercier, J. Luc, I. Rau, F. Kajzar, B. Sahraoui, *Adv. Mat.* **20**, 1013 (2008).
- [6] J. Roncali, *Chem. Rev.*, **92**(4), 711 (1992).
- [7] P.N. Prasad, J. Swiatkiewicz, J. Pfleger, *Mol. Cryst. Liq. Cryst.*, **160**(1), 53 (1988).
- [8] V. H. Houlding, A. Hahata, J.T. Yardley, R. L. Elsenbaumer, *Chem. Mat.*, **2**(2), 169 (1990).
- [9] W. N. Herman, L.M. Hayden, *J. Opt. Soc. Am. B*, **12**(3), 416 (1995).
- [10] U. Gubler, C. Bosshard, *Phys. Rev. B* **61**(16), 10702 (2000).
- [11] F. Kajzar, Y. Okada-Shudo, C. Meritt, Z. Kafafi, *Synth. Met.*, **117**, 189 (2001).
- [12] R.N. Adams, *Acc. Chem. Res.* **2**, 175 (1969).
- [13] E. Genies, G. Bidan, A.F. Diaz, *J. Electroanal. Chem.*, **149**(1-2), 101 (1983).
- [14] J. F. Ambrose, R.F. Nelson, *J. Electrochem. Soc.*, **115**(11), 1159 (1968).
- [15] G. J. Lee, S. W. Cha, S. J. Jeon, J. I Jin, J. S. Yoon, *J. Korean Phys. Soc.*, vol. 39, n. 5, pp. 912-915.
- [16] R.A. Myers, N. Mukherjee, S. R. J. Brueck, *Opt. Lett.*, **16**(22), 1732 (1991).
- [17] B. Sahraoui, X. Nguyen Phu, M. Sallé, A. Gorgues *Optics Letters*, **23**(23), 1811 (1998).
- [18] N. Terkia-Derdra, R. Andreu, M. Sallé, E. Levillain, J. Orduna, J. Garin, E. Orti, R. Viruela, R. Pou-Amérigo, B. Sahraoui, A. Gorgues, J.-F. Favard, A. Riou, *Electrochemical Properties Chemistry - A European Journal*, **6**(7), 1199 (2000).
- [19] K. Kubodera, H. Kobayashi, *Mol. Cryst. Liq. Cryst.*, **182**(1), 103 (1990).
- [20] F. Kajzar, J. Messier, *Phys. Rev.* **32**(4), 2352 (1985).

* Corresponding author: bouchta.sahraoui@univ-angers.fr